References

1. A. J. Broderick, in *Proceedings of the Second Conference on the Climatic Impact Assessment Program, November 14–17, 1972* (Publication DOT-TSC-OST-73-4, National Technical Information Service, Springfield, Va., 1973).
2. P. Cutchis, *Science* **184**, 13 (1974).
3. J. V. Dave and P. M. Furukawa, *Meteorol. Monogr.* **7** (No. 29), 1 (1966).
4. B. E. Johnson, F. Daniels, Jr., I. A. Magnus, in *Photophysiology, Current Topics*, A. C. Giese, Ed. (Academic Press, New York, 1968), vol. 4, p. 139.
5. J. N. Howard, J. I. F. King, P. R. Gast, in *Handbook of Geophysics* (Macmillan, New York, 1961), chap. 16.
6. N. Braslau and J. V. Dave, *Reports RC 4114, 4152, 4308* (IBM T. J. Watson Research Center, Yorktown Heights, N.Y., 1972–1973). See also N. Braslau and J. V. Dave, *J. Appl. Meteorol.* **12**, 601 (1973); *ibid.*, p. 616.
7. R. A. McClatchey, R. W. Fenn, J. E. A. Selby, J. S. Garing, F. E. Volz, *Rep. No. AFCRL-70-0527* (Air Force Cambridge Research Laboratories, Bedford, Mass., 1970).
8. D. Deirmendjian, *Electromagnetic Scattering on Atmospheric Polydispersions* (Elsevier, New York, 1969).
9. C. E. Junge, *Air Chemistry and Radioactivity* (Academic Press, New York, 1963).
10. J. V. Dave and N. Braslau, in preparation.
11. E. Raschke and W. R. Bandeen, *J. Appl. Meteorol.* **9**, 215 (1970).
12. J. T. Twitty and J. A. Weinman, *ibid.* **10**, 725 (1971).
13. J. V. Dave and J. Canosa, *J. Atmos. Sci.* **31**, 1089 (1974); J. V. Dave, *Rep. No. UCRL-51581* (Lawrence Livermore Laboratory, University of California, Livermore, 1974).
14. P. Halpern, thesis, University of California, Davis, in preparation.

23 August 1974

Skylab Radar Altimeter: Short-Wavelength Perturbations Detected in Ocean Surface Profiles

Abstract. *Short-wavelength anomalies in sea surface topography, caused by the gravitational effects of major ocean bottom topographic features, have been detected by the radar altimeter aboard Skylab. Some features, such as deep ocean trenches, seamounts, and escarpments, displace the ocean surface by as much as 15 meters over 100-kilometer wavelengths. This experiment demonstrates the potential of satellite altimetry for determining the ocean geoid and for mapping major features of the ocean bottom.*

We report here preliminary results from the Skylab radar altimeter which was part of the Earth Resources Experimental Package (EREP) aboard Skylab. This was the first in a series of altimeters planned to be placed in Earth orbit to determine both geodetic and oceanographic characteristics of the ocean surface. The primary purposes of the radar altimeter experiment were to determine the feasibility of using satellite altimetry to investigate geophysical phenomena and to obtain the necessary engineering data for the design of future satellite altimeter systems.

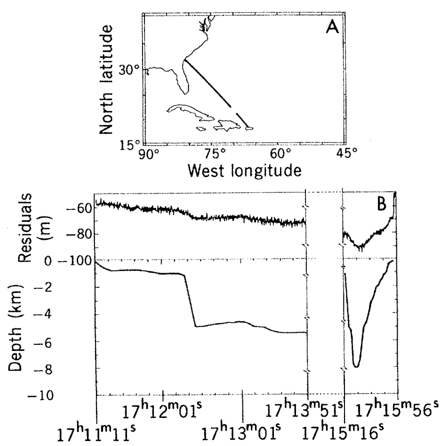

Fig. 1. (A) Subsatellite trace for EREP pass 4, SL-2, 4 June 1973. (B) Sea surface topography determined by altimeter, and the bottom topography beneath the subsatellite trace, showing the Blake Escarpment and the Puerto Rico Trench.

Skylab was placed into Earth orbit on 14 May 1973 at a mean altitude of 440 km and an inclination of 50 deg. More than 150 altitude data sets have been acquired during the three manned Skylab missions (SL-2, SL-3, and SL-4), and data gathered from SL-2 and SL-3 provide the data base for this investigation.

The radar altimeter was built by the General Electric Company, Ithaca, New York. It operates at a 13.9-Ghz frequency, transmits one of three selectable pulsewidths (20, 100, or 10 nsec) at a pulse repetition rate of 250 pulses per second, and has five different operating modes, three of which provide altitude measurements. The altitude data are recorded at a rate of eight samples per 1.04 seconds. Other characteristics of the altimeter are described in McGoogan (*1*) and McGoogan *et al.* (*2*).

The basic concept of altimetry is the utilization of a highly stable, moving reference system from which vertical measurements to the ocean surface are made. The orbiting Skylab, positioned by ground-tracking instrumentation, provides the stable reference surface, and the radar altimeter measures the distance from the reference orbit to the sea surface. The altimeter is basically a conventional tracking radar which tracks in range only. A narrow pulse is transmitted from the altimeter to the sea surface. The time interval from the transmit time to the half-power point of the leading edge of the return pulse is proportional to the altitude. These transmit times are measured with a closed-loop tracking system with bandwidths of a few hertz to follow the dynamics of the ocean surface. If the pulsewidth represents a time spread on the ocean surface that is less than the beamwidth, then either pulsewidth, sea state, or both will determine the footprint size. This footprint acts as a spatial filter that must be considered in analyzing surface features.

Factors considered in the calibration of the altitude measurements include the pointing of the antenna, pulsewidth or bandwidth changes (or both), in-flight calibration data, and atmospheric retardation. Prior to in-depth analysis, antenna pointing is assured to be within 0.5 deg of the nadir, since pointing errors produce bias errors in the altitude measurement. Altitude biases up to 15 m due to the switching of transmitted pulsewidths or receiver bandwidths, or both, are corrected for in the processing. The alti-

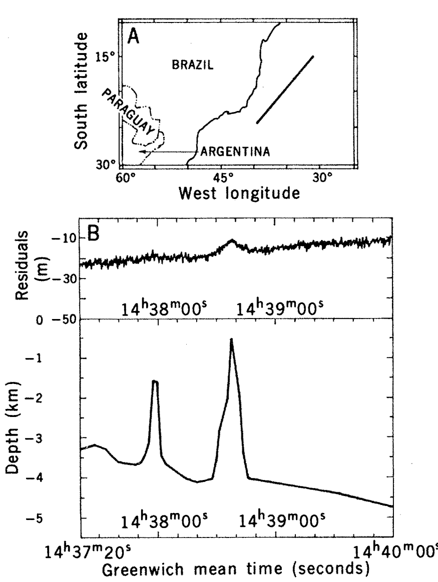

Fig. 2. (A) Subsatellite trace for EREP pass 11, SL-3, 2 September 1973. (B) Sea surface topography determined by altimeter, and the bottom topography beneath the subsatellite trace, showing seamounts off the east coast of Brazil.

tude measurement stability is monitored by measuring a fixed time delay line within the altimeter system. The bias of this calibration has been consistently less than 20 cm over a 4-month period. Finally, to establish a more absolute comparison with geoids measured with other techniques, a constant tropospheric refraction correction of 2.79 m was subtracted from each altitude measurement.

The Skylab orbital positions were estimated by an orbit determination program with the use of unified S-band (USB) range and range rate tracking data obtained from the Goddard Space Flight Center. Because of the large drag effect on the spacecraft and the thrusting used for spacecraft maneuvers, the lengths of the orbital solutions were minimized, resulting in an uncertainty in the calculated orbital height of about 25 m.

A major preliminary result of an altimeter-sensed ocean profile is shown in Fig. 1. Data were acquired from EREP pass 4, SL-2, on 4 June 1973, when Skylab was passing from a point off the east coast of South Carolina to a point just south of Puerto Rico, as shown in Fig. 1A. The difference between the altitude calculated to the ellipsoid ($a = 6,378,155$ m, $f = 1/298.255$, where a is the length of the semimajor axis and f is the flattening of the ellipsoid) and the altitude measured by the altimeter to the ocean surface is shown in Fig. 1B. A bottom topography profile along the subsatellite trace, derived from Pratt (*3*), is shown in Fig. 1B. Note the 4-m drop in the ocean surface profile over the Blake Escarpment, the low-frequency rise at abyssal plain area, and the 15-m depression in the ocean surface over the Puerto Rico Trench, a 100-km wavelength feature. The relative disagreement of the minima of the two profiles over the trench can be explained in terms of local gravity conditions. Bowin *et al.* (*4*) observed a similar disagreement over the trench minima between the free-air anomaly and water depth measurements. Moreover, the difference in slope between the north and south flanks of the trench are clearly evident in the altitude residuals. Von Arx (*5*) and Stanley *et al.* (*6*), using independent techniques, have estimated ocean profile depressions of 17.5 and 22.5 m, respectively, across different sections of the trench.

Figure 2 depicts a similar comparison of data from EREP pass 11, SL-3, taken on 2 September 1973, just off the east coast of Brazil over the South Atlantic. The ground track for the pass is shown in Fig. 2A. The altimeter measurement residuals from the USB-determined orbit in Fig. 2B show an interesting anomaly in the ocean surface profile. Comparing the anomaly with the ocean bottom topography derived from Uchupi (*7*), also presented in Fig. 2B, we see a distinct correlation of the second seamount with the high-frequency signature from the altitude residuals. The first seamount does not have as great an effect on the sea surface because it has less mass and is not part of a seamount chain as is the second seamount. In addition to these specific results, the Mid-Atlantic Ridge, the Cape Verde Islands, the Mid-American Trench, and the Flemish Cap have each had a detectable influence on the altimeter-sensed ocean surface topography.

In conclusion, we feel that the Skylab altimeter has significantly demonstrated an ability to detect and map even short-wavelength undulations in the ocean geoid. In addition, these short-wavelength undulations are often highly correlated with major ocean bottom topography. Therefore, the potential of satellite altimeters for charting mass density distributions and for contributing to the understanding of the earth's geological structure can easily be recognized.

C. D. LEITAO
J. T. MCGOOGAN
National Aeronautics and Space Administration, Wallops Flight Center, Wallops Island, Virginia 23337

References and Notes

1. J. T. McGoogan, paper presented at the Institute of Electrical and Electronics Engineers International Convention and Exposition, New York, March 1974.
2. J. T. McGoogan, L. S. Miller, G. S. Brown, G. S. Hayne, *Proc. Inst. Elec. Electron. Eng.* **62**, 793 (1974).
3. R. M. Pratt, *Atlantic Continental Shelf and Slope of the United States: Physiography and Sediments of the Deep-Sea Basin* (Government Printing Office, Washington, D.C., 1968), plate 1.
4. C. O. Bowin, R. Bernstein, E. D. Ungar, J. R. Madigan, *Inst. Elec. Electron. Eng. Trans. Geosci. Electron.* **GE-5**, 2 (1967).
5. W. S. von Arx, *Science* **154**, 1651 (1966).
6. H. R. Stanley, C. F. Martin, N. A. Roy, A. G. Mourad, paper presented at 15th General Assembly of the International Union of Geodesy and Geophysics, Moscow, August 1971.
7. E. Uchupi, "Bathymetric atlas of the Atlantic, Caribbean, and Gulf of Mexico" (unpublished manuscript, Reference No. 71-72, Woods Hole Oceanographic Institution, Woods Hole, Mass., December 1971).
8. We thank W. T. Wells for assistance in the orbital analysis, T. D. Sommers and V. E. Hopkins for programming support, W. Speidel for technical support, and the referees for their helpful suggestions.

15 July 1974; revised 30 September 1974

Electron Imaging of Pyrrhotite Superstructures

Abstract. *Natural pyrrhotites, when studied by high resolution electron microscopy, yield crystallographic information on a unit cell scale. Structural heterogeneity is prominent. The many reported superstructures are interpretable through an antiphase model. The 5C pyrrhotite superstructure results from an ordered sequence of antiphase domains while the higher temperature* NC *type results from a disordered sequence.*

Pyrrhotite, $Fe_{1-x}S$, is a geologically interesting, industrially important, and crystallographically complex mineral. It has commonly been used as a type example of nonstoichiometry. At low temperatures, however, it appears to consist of a series of chemically and structurally discrete phases related by superstructuring. In spite of extensive studies, a number of problems persist: (i) there is confusion regarding the exact number and stabilities of its many reported superstructures, (ii) detailed information on the mechanism of superstructure formation is lacking, and (iii) there is apparently a direct relation between the length of the superstructure in the c-direction and the composition (*1*), but the nature of this relation is not yet clear (*2*).

Detailed structural information on a unit cell level has been obtained for silicate minerals by using high resolution electron microscopy (*3, 4*). It was thought that electron microscopy would provide information pertinent to the problems of pyrrhotite superstructuring beyond that obtainable by x-ray techniques. A successful study of pyrrhotite would also indicate the applicability of high resolution electron microscopy to structure problems of other sulfides.

Cell dimensions of pyrrhotite super-